Macromolecules

ARTICLE

pubs.acs.org/Macromolecules

Evolution of the Environment of Guest Molecules in Dynamically Heterogeneous Matrices of Poly(ethyl methacrylate) and Poly(*n*-butyl methacrylate) Far below T_g

S. Yu. Grebenkin* and V. M. Syutkin

Institute of Chemical Kinetics and Combustion, Novosibirsk, 630090, Russian Federation

ABSTRACT: Photoinduced *cis*−*trans* isomerization has been used to measure the lifetime of structural heterogeneities in the matrices of poly(ethyl methacrylate) (PEMA) and poly(*n*-butyl methacrylate) (P*n*BMA) far below T_g. Nonequilibrium distribution of probe molecules over their environments was formed by a partial *trans* → *cis* isomerization. To monitor the equilibration process, the back-isomerization was started after different delay times. The change in quantum yield of back-isomerization with delay time is interpreted to result from the change in the environment of probe molecules. The times required for the environments to change were estimated over a temperature range of T_g − 113 K to T_g − 73 K for PEMA and T_g − 65 K to T_g − 25 K for P*n*BMA. It was found that the lifetimes of different environments differ from each other by up to 2 orders of magnitude and correlate with the isomerization probability: the environment of the molecules which isomerize faster changes more often. For both matrices, the value of 55 kJ/mol was estimated for the activation energy of the lifetime of the least mobile environments while the lifetime of the most mobile environments depends on temperature only weakly.

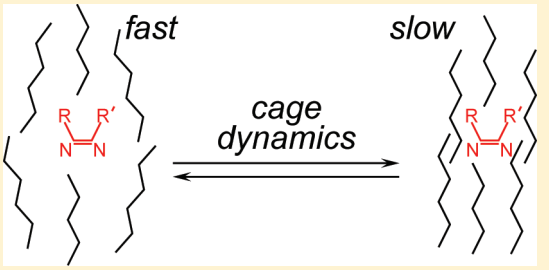

INTRODUCTION

The dynamic properties of disordered substances and, particularly, of amorphous polymers are of considerable scientific interest and of practical importance. To date, it is established that the dynamics in supercooled liquids is spatially heterogeneous, which means that the characteristic times of molecular motion in different regions of a matrix differ from each other.[1−3] Spatially heterogeneous dynamics can be the consequence of fluctuations present in any equilibrium liquid.[4−8] The typical size of the regions of different mobility falls in the range from 1 to 3.5 nm for various glass-formers.[8−12] It has been proved that the dynamical characteristics of a region do not remain constant but change in time: the region of high mobility can transform into the region of low mobility and vice versa.[13−21] The average period during which the dynamic properties of a region do not change is called the exchange time.[22]

The exchange dynamics was measured in low-molecular-weight and polymeric substances using the photobleaching technique,[22−24] the method of multipulse nuclear magnetic resonance,[14−16,18,20] single molecule spectroscopy,[25−29] and other methods.[21,30−33] The obtained values of exchange time are comparable with the time of α-relaxation or exceed it up to several orders of magnitude which is explained, most probably, by the large size of probe molecules.[27] Mainly, the studies were performed at or above the glass transition temperature.

Only a few works reported the results of measuring the exchange dynamics in polymers. The exchange times were measured in polystyrene,[16,24] poly(vinyl acetate),[14,21,27] and poly(methyl acrylate).[26] As far as we know, below T_g, the measurements of exchange dynamics were carried out only in poly(vinyl acetate) (down to T_g − 10 K[21] and at T_g − 1 K[27]).

Isomerization reactions in polymer matrices had been studied for a long time,[34] mainly due to their practical significance. Also, they were used as probe processes in exploring the dynamic characteristics of polymeric materials.[35−40] Typically, the kinetics of the reactions in polymers reflects matrix heterogeneity.

The goal of present study was to investigate the exchange dynamics in two polymeric matrices, PEMA and P*n*BMA, far below T_g using *cis*−*trans* photoisomerization of guest molecules as a probe process. Earlier,[41] utilizing this approach, it has been found that, in glassy *o*-terphenyl, the time required for the environment to change is close to the rotational time of the probe molecules and follows the temperature dependence of α-relaxation time. Because of the chain molecular structure, the relaxation behavior of polymers differs noticeably from that of small molecule glass-formers.[42−45] Therefore, we can expect that the exchange dynamics in polymers also differs from that in low molecular weight glasses.

The first question was: does the exchange dynamics persist far below T_g in polymers? If it does, then the second question arises: what kind of polymer dynamics does govern the exchange in polymers at such low temperatures?

EXPERIMENTAL SECTION

Sample Preparation. 1-Naphthyl-*p*-azomethoxybenzene (NAMB) was synthesized in our laboratory in accordance with ref 46 and used after

Received: January 12, 2011
Revised: March 25, 2011
Published: May 03, 2011

dx.doi.org/10.1021/ma2000042 | *Macromolecules* 2011, 44, 4538–4545

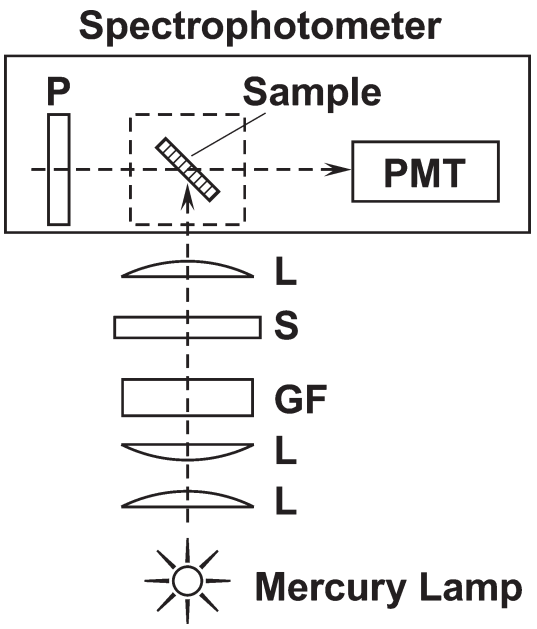

Figure 1. Schematic representation of the experimental setup. L, lens; S, shutter; GF, glass filters; P, polarizer; PMT, photomultiplier tube.

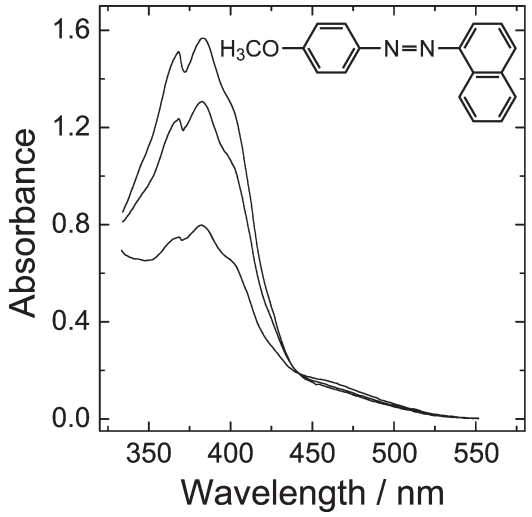

Figure 2. UV−vis absorption spectrum of NAMB in P*n*BMA before irradiation (top curve), after 15 s of irradiation with the light of 405 nm (bottom curve), and the steady-state spectrum resulting from the long irradiation with the light of 546 nm (middle curve), 263 K. The inset shows the chemical structure of NAMB.

thin-layer chromatographic purification. The inset in Figure 2 shows its chemical structure. PEMA (M_w = 515 000 by GPC, T_g = 63 °C) and P*n*BMA (M_w = 337 000 by GPC, T_g = 15 °C) were purchased from Aldrich.

Polymer films were prepared in the following way. NAMB solution in chloroform (≥99.0%, JSC EKOS-1) with the concentration of 0.016% w/v was added to polymer/chloroform solution with the concentration of 5.7% w/v and stirred for 1 h. The amount of NAMB was about 0.045 wt % of polymer. The resulting solution was dropped on a glass plate and dried for 20 min at room temperature. The obtained polymer film was removed from the plate and dried under vacuum for 5 h at 313 K (P*n*BMA) or 343 K (PEMA).

Then seven rectangular pieces (8 × 20 mm^2, the thickness of 25 ± 5 μm) of the film were put together and clamped between two quartz plates. Prior to measurements, the samples were stored in dark in air at room temperature for 6 months.

Kinetic Measurements. The kinetics of *cis*−*trans* isomerization was monitored by measuring the sample absorbance (spectrophotometer Specord UV−vis, Carl Zeiss Jena) at the wavelength of the absorption maximum of *trans* isomer (382 nm).

The experimental setup is represented schematically in Figure 1. A 500 W high-pressure mercury arc lamp (DRSh-500−2M) operating on direct current was used for irradiation. The time stability of light flux was ±1%. The required lines of the mercury spectrum (405 and 546 nm) were isolated using standard sets of colored glass filters immersed into water bath. The photon flux measured with the optical power meter (Thorlabs PM120) at 546 nm was (1.8 ± 0.2) × 10^{17} photons s^{-1} cm^{-2}. The light absorption by the sample at 546 nm did not exceed 1%; therefore, the light intensity was considered constant throughout the sample.

The sample was placed into the temperature-controlled (Polikon 613, temperature controller, Thermex, St. Petersburg) cell cooled with gaseous nitrogen and equipped with quartz windows. The sample temperature was kept constant to within 0.1 K with the measuring accuracy of ±0.5 K. The polymer films were oriented at an angle of 45° both to the irradiation and the probe beams (see Figure 1).

Light-induced *cis*−*trans* isomerization of azo-compounds in glassy matrices is often accompanied by their orientation.[34] In order to obtain the isomerization kinetics, we have recorded the absorption of both horizontally ($Abs_\perp$) and vertically ($Abs_\parallel$) polarized probe light. The combination

$$\mathrm{Abs}(t) = \frac{\mathrm{Abs}_\perp(t) + 2\mathrm{Abs}_\parallel(t)}{3} \quad (1)$$

provides the value which is independent of angular particle distribution and proportional to the isomeric composition. Hereafter, the term absorbance denotes the value determined in accordance with eq 1.

To polarize probe light, the polarizer (LOMO PLC) coupled with the step motor (Electroprivod Ltd., St. Petersburg) was installed inside the spectrophotometer. A homemade mount allows two fixed positions of the polarizer at which the probe light has either vertical or horizontal polarization. For a time of absorbance measurement, the irradiation was interrupted by a homemade optical shutter with a closing (opening) time of 27 ms.

Figure 2 shows the optical absorption spectra of NAMB in P*n*BMA in dark and after irradiation with light of different wavelengths. The difference in the spectra is due to different isomer contents.

Experiment Routine. Before each measurement, the samples were warmed up above T_g: the films of P*n*BMA were warmed up for 1 h at 313 K (T_g + 25 K) and the films of PEMA for 0.5 h at 353 K (T_g + 17 K). As a result of warming, the azo-compound was completely converted into the *trans*-form. Then the samples were aged for 1 h at T_g − 6 K and cooled to the temperature of measurement at a rate of about 2 K/min. In accordance with the results of dielectric measurements,[42] at T_g − 6 K, the times of α-relaxation are about 300 s for PEMA (estimated by extrapolation of the data) and 600 s for P*n*BMA. Structural relaxation slows down strongly as the temperature decreases; therefore, we believe that the matrix structure changes only slightly during cooling.

Then the samples were preirradiated at measurement temperature with the light of 405 nm for 15 s to convert about 50% of NAMB into the *cis*-form. The kinetics of *cis* → *trans* isomerization induced by light of 546 nm was measured following the different dark pauses, τ_{dark}, after the preirradiation with 405 nm light.

The rate of dark *cis* → *trans* isomerization is negligible in the temperature range studied.

dx.doi.org/10.1021/ma2000042 |*Macromolecules* 2011, 44, 4538–4545

BACKGROUND OF THE METHOD

In this section, we describe the method used to determine the environment lifetime. Because of a difference in the environment, the probability to isomerize is different for different molecules. The principle of the method consists in generating the most reactive *cis*-molecules ("fast" molecules) and subsequent monitoring their reactivity change.

Selective generation of fast *cis*-molecules is possible owing to the correlation of the rates of *trans* $\xrightarrow{h\nu_1}$ *cis* and *cis* $\xrightarrow{h\nu_2}$ *trans* isomerizations of NAMB in polymer matrix. Earlier, the correlation of the rates of forward and backward reactions was reported for merocyanine $\leftrightarrow$ spiropyran conversions in poly(propyl methacrylate).[38] Since, at first, the fast *trans*-molecules are converted into *cis*-ones, the partial *trans* $\xrightarrow{405\text{nm}}$ *cis* isomerization results mainly in the formation of fast *cis*-molecules. In the dark, with time, the environment of *cis*-molecules changes, which leads to a decrease in the rate of subsequent *cis* $\xrightarrow{546\text{nm}}$ *trans* isomerization.

In the case if the irradiation with light of 546 nm results in complete conversion of azo compound into the *trans*-form, we can generate fast *cis*-molecules just by preirradiation with the light of 405 nm for any short period, τ_{405}. In that case, the dependence of the kinetics of *cis* $\xrightarrow{546\text{nm}}$ *trans* isomerization on the initial content of *cis*-isomer is monotonous: the more *cis*-molecules are generated, the slower the kinetics is.

In reality, irradiation with light of 546 nm results in incomplete conversion of the probe into the *trans*-form (a steady state fraction of *trans*-isomer is about 85%). Therefore, the dependence of the kinetics of isomerization induced by light of 546 nm on the time of preirradiation (405 nm) is more complicated. In this case, to understand how the kinetics of *cis* $\rightarrow$ *trans* isomerization depends on τ_{405}, it is helpful to consider a model system of two ensembles: the one of fast and the other of slow molecules. When the sample is irradiated with the light of 546 nm, its absorbance follows the equation

$$\mathrm{Abs}(t) = \mathrm{Abs}_{\mathrm{f,eq}} + \mathrm{Abs}_{\mathrm{s,eq}} + (\mathrm{Abs}_{\mathrm{f}}(0) - \mathrm{Abs}_{\mathrm{f,eq}})\mathrm{e}^{-k_{\mathrm{f}}t} + (\mathrm{Abs}_{\mathrm{s}}(0) - \mathrm{Abs}_{\mathrm{s,eq}})\mathrm{e}^{-k_{\mathrm{s}}t} \quad (2)$$

where $\mathrm{Abs}_i(0)$ and $\mathrm{Abs}_{i,\mathrm{eq}}$ are the starting and photoequilibrium absorbance values, k_i are the effective rate constants (i = f, s), and the indexes f and s stand for fast and slow.

Equation 2 shows that the isomerization kinetics depends essentially on the starting absorbances, $\mathrm{Abs}_{\mathrm{f}}(0)$ and $\mathrm{Abs}_{\mathrm{s}}(0)$. The starting absorbances, in their turn, are given by the preirradiation time, τ_{405}. Three different intervals of τ_{405} can be marked out:

(1) From 0 to the moment $t_{\mathrm{f,eq}}$ when the absorbance of fast molecules, $\mathrm{Abs}_{\mathrm{f}}(0)$, reaches the value $\mathrm{Abs}_{\mathrm{f,eq}}$; an increase in τ_{405} within this interval leads to slowing down of change in the absorbance induced by the light of 546 nm (because the value of $\mathrm{Abs}_{\mathrm{f}}(0) - \mathrm{Abs}_{\mathrm{f,eq}}$ decreases to a greater extent than the $\mathrm{Abs}_{\mathrm{s}}(0) - \mathrm{Abs}_{\mathrm{s,eq}}$).

(2) From $t_{\mathrm{f,eq}}$ to the moment $t_{\mathrm{s,eq}}$ when the absorbance of slow molecules $\mathrm{Abs}_{\mathrm{s}}(0)$ reaches the value $\mathrm{Abs}_{\mathrm{s,eq}}$; an increase in τ_{405} within this interval causes an acceleration of the subsequent absorbance change caused by the light of 546 nm due to both an increase in the "fast" portion of absorbance and a decrease in the "slow" one.

(3) Further increase in preirradiation time from the moment $t_{\mathrm{s,eq}}$ to infinity again causes slowing down of the absorbance change under 546 nm light due to an increase in the "slow" portion of absorbance. The "fast" portion is not increasing noticeably further on because it has come close to the steady state level. Note that this consideration is valid for the case of strong difference in the isomerization times of slow and fast molecules.

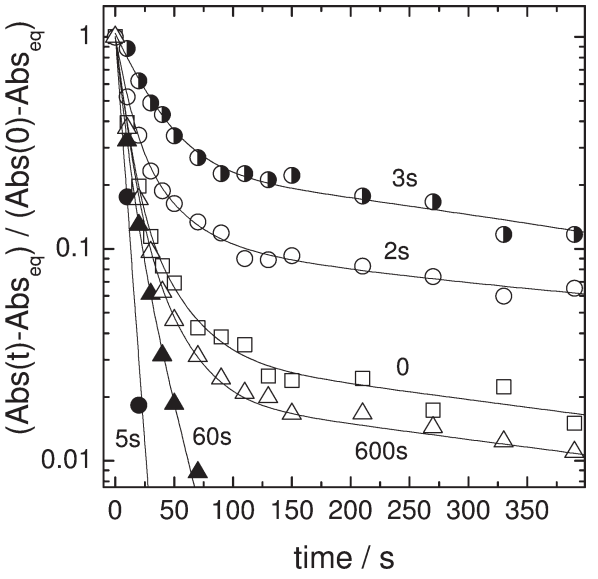

Figure 3. First-order plot for the kinetics of photoisomerization (546 nm) of NAMB in P*n*BMA following different periods of preirradiation with the light of 405 nm, τ_{405}. The values of τ_{405} are listed in the figure, τ_{dark} = 15 s, T = 253 K. The lines are guides for the eye.

Figure 3 shows the kinetics of light-induced (546 nm) isomerization of NAMB in P*n*BMA following different periods of preirradiation with the light of 405 nm. The presented results are in good agreement with the model described above. Actually, at short τ_{405}, an increase in τ_{405} causes slowing down of the absorbance change (compare curves "0", "2s", and "3s"). As τ_{405} increases further, the 546 nm isomerization accelerates strongly (curve "5s"). Further increase in τ_{405} leads to slowing down of the isomerization again (the curves "60s" and "600s"). After 600 s of irradiation with the light of 405 nm, the isomer ratio is equal to a steady-state one. The closeness of the curves "0" and "600s" most likely witnesses that the steady-state isomer ratios inside the "fast" and "slow" ensembles are close to each other.

To measure the exchange dynamics, the nonequilibrium distribution of probes is created by the 405 nm preirradiation of the sample for 15 s. After preirradiation, the isomer ratio inside the ensemble of slow molecules is close to the steady-state one, resulting from the irradiation with the light of 546 nm. Therefore, immediately after preirradiation, the slow molecules do not manifest themselves in the kinetics of subsequent 546 nm induced isomerization; only the isomerization of fast molecules results in the change of absorbance. With time, due to the exchange between the slow and fast ensembles, the equilibrium distribution is established. This results in slowing down of subsequent isomerization induced by the 546 nm irradiation. The exchange times were estimated from the set of curves obtained at different τ_{dark} using computer modeling.

RESULTS AND DISCUSSION

Dependence of Isomerization Kinetics on Dark Interval after the Formation of *Cis*-Molecules. Figure 4 shows typical

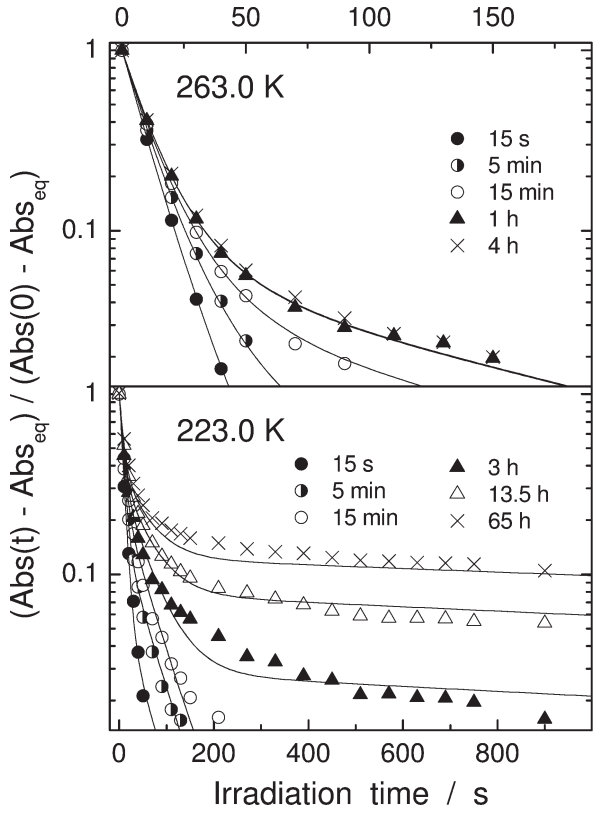

Figure 4. First-order plot for the kinetics of photoinduced (546 nm) isomerization of NAMB in P*n*BMA following different dark intervals after formation of *cis*-molecules. The values of τ_{dark} are listed in the figure. Solid lines are the results of fitting the data with the model of gradual changes in the environment.

kinetic curves for the *cis* $\overset{546nm}{\rightarrow}$ *trans* isomerization of NAMB in P*n*BMA following different dark intervals, τ_{dark}, after 15 s preirradiation with light of 405 nm. Isomerization slows down strongly with an increase in τ_{dark}. At 223 K, the time of isomerization [considered here as the time required for the value $(\mathrm{Abs}(t) - \mathrm{Abs}_{eq})/(\mathrm{Abs}(0) - \mathrm{Abs}_{eq})$ to reach 0.98] after the dark interval of 65 h amounts to 3 h while after the pause of 15 s it does not exceed 1 min.

In the framework of dynamical heterogeneity concept, a decrease in the quantum yield of *cis* → *trans* isomerization with an increase in dark interval is due to the change in the environments of NAMB molecules. Two different phenomena can be reasons of this change.

The first one is the change in the local environment caused by the exchange processes. This means that with time, due to the exchange, the initial (nonequilibrium) distribution of probe molecules over their environments comes to equilibrium.

The second possible reason can be a local structural relaxation of the matrix *caused* by the *trans* → *cis* isomerization. The environment of new-born *cis*-molecule is considered to be "adjusted" to the geometry of *trans*-molecule. Therefore, immediately after the formation of *cis*-molecule, the probability of *cis* → *trans* conversion is the highest. Because of the structural relaxation, the matrix adjusts to the geometry of *cis*-molecule. In the course of relaxation, the quantum yield of *cis* → *trans* isomerization decreases and reaches a minimum when the matrix becomes adjusted to the *cis*-molecule.

To choose between these two alternatives, two additional experiments were carried out. The step-by-step scheme of the

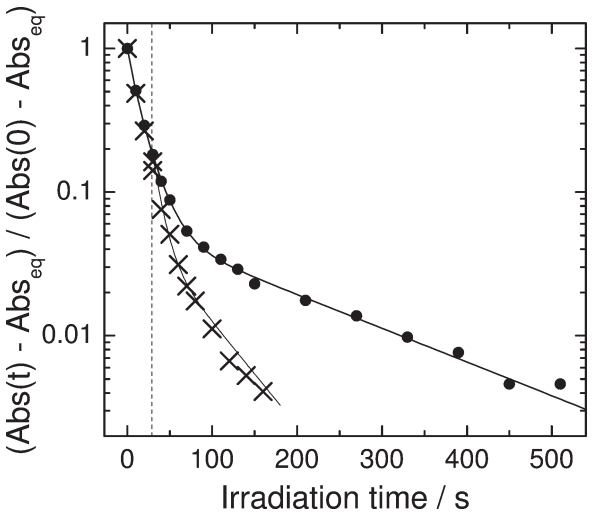

Figure 5. Evidence of the exchange process. The kinetics of continuous (solid circles) and interrupted (crosses) photoinduced (546 nm) isomerization of NAMB in P*n*BMA. The vertical dotted line marks the moment of interruption of the irradiation; after keeping the sample in the dark for 2 h, the irradiation was continued. $T = 263$ K, $\tau_{dark} = 2$ h. The lines are guides for the eye.

first experiment is as follows. At 263 K, the P*n*BMA sample was irradiated with the light of 405 nm for 15 s and stored in dark for 2 h to bring the molecular distribution over environments to an equilibrium. Then the sample was irradiated with the light of 546 nm for 30 s to convert fast *cis*-molecules into the *trans*-ones and stored in the dark for 2 h. Then photoisomerization (546 nm) was resumed. In such a way, the test kinetics of *cis* $\overset{546nm}{\rightarrow}$ *trans* isomerization was obtained.

Figure 5 shows the test kinetics (crosses) together with the standard kinetics recorded without interruption of irradiation (solid circles). One can see that keeping of the sample in dark after partial *cis* $\overset{546nm}{\rightarrow}$ *trans* conversion leads to the acceleration of isomerization. The result of this experiment proves that the exchange is the reason for a decrease in the rate of isomerization with an increase in τ_{dark}. Actually, the exchange occurring in the dark after interruption of isomerization leads to the restoration of molecular distribution and, thereby, to the appearance of fast molecules while the relaxation would lead only to slowing down of isomerization.

Figure 3 suggests the idea of the second experimental proof of the exchange processes. The figure shows that after 3 s of preirradiation with the light of 405 nm the isomerization induced by the light of 546 nm proceeds slowly. We found that, in this case, an increase in τ_{dark} leads to an acceleration of the 546 nm induced isomerization. After the dark period of 10 h, the kinetic curve becomes an equilibrium one, no further change was detected. It was established that the equilibrium curves recorded after 3 and 15 s of 405 nm preirradiation coincide. Recall that in the case of "15 s of 405 nm preirradiation" an increase in τ_{dark} leads to slowing down of the isomerization. The obtained results are quite consistent with the exchange model and demonstrate that the exchange processes lead to the same (equilibrium) distribution of the probes over environments independently of their initial distribution.

In addition, the influence of sample aging at temperature of measurement prior to generation of *cis*-molecules on the kinetics

dx.doi.org/10.1021/ma2000042 |*Macromolecules* 2011, 44, 4538–4545

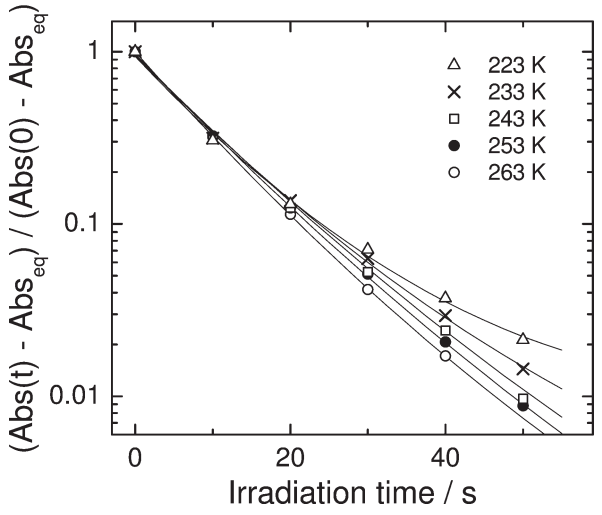

Figure 6. First-order plots for photoinduced (546 nm) isomerization of NAMB in P*n*BMA following 15 s dark pause after preirradiation with light of 405 nm.

of subsequent isomerization was studied. It was found that aging for the period equal to the highest dark interval at a given temperature has no effect on the kinetics.

Temperature Dependence of Isomerization Kinetics. Figure 6 demonstrates the kinetics of *cis* → *trans* isomerization following a minimum dark interval (15 s) at different temperatures. The isomerization kinetics depends on temperature very weakly in the range studied. The presented curves reflect the isomerization of the fastest *cis*-molecules. We interpret this result to mean that temperature has only a slight effect on the probe isomerization in loose environments.

The presented kinetic curves are nearly exponential. Hence, the *cis*-molecules that are revealed in the kinetics of *cis* → *trans* isomerization are kinetically equivalent. By contrast, the equilibrium kinetic curve (recorded after long dark intervals) strongly depends on temperature (cf. top curves in Figure 4 at 223 and 263 K). We assume that the strong temperature dependence is caused by the temperature dependence of the isomerization rate of slow molecules. An additional experiment was done to confirm this assumption.

The film of NAMB/P*n*BMA was preirradiated with the light of 405 nm for 15 s at 263 K and kept for 2 h in dark. During this period, the equilibrium distribution of probe molecules over their environments is established (see top panel of Figure 4). Then the sample was cooled for 15 min to 243 K (the time required to reach an equilibrium distribution at any temperature below 263 K much exceeds 15 min) and the reference kinetics of $cis \xrightarrow{546\text{nm}} trans$ isomerization was measured. The reference kinetics coincides with the equilibrium kinetics of isomerization in the sample preirradiated at 243 K. On the basis of that, we conclude that the temperature dependence of equilibrium kinetics originates from the temperature dependence of the isomerization rate of slow molecules.

Modeling of Environment Evolution. To simulate the *cis* → *trans* isomerization kinetics, we used a discrete distribution of probe molecules over effective rate constants of isomerization, k_i. The distribution of probes over k_i reflects their distribution over different environments. We have restricted ourselves to the probe distribution over four ensembles as a smaller number of ensembles is not sufficient to describe the full set of kinetic curves (at all dark pauses) below 253 K. The ensembles were enumerated from 1 to 4 (the larger index corresponds to the slower molecules). Because of the change in environment, molecules transit between the ensembles. The probability of the transition from the *i*th to the *j*th ensemble is denoted by W_{ij}.

The values of W_{ij} were found from the numerical solution of the system of differential equations

$$\frac{dC_i(t)}{dt} = -k_iC_i(t) - \sum_j W_{ij}C_i(t) + \sum_j W_{ji}C_j(t) \qquad (3)$$

which provides the best coincidence between the calculated and experimental kinetic curves for all the curves obtained at a given temperature. Here, $C_i(t)$ is the population of the *i*th ensemble. The equation

$$\frac{\mathrm{Abs}(t) - \mathrm{Abs}_\infty}{\mathrm{Abs}(0) - \mathrm{Abs}_\infty} = \frac{C(t) - C_\infty}{C(0) - C_\infty}$$

where $C \equiv \Sigma C_i$ allows us to compare directly simulation results with the experimental data.

It was taken that, immediately after preirradiation, only the values of $C_1(t)$ and $C_2(t)$ are not equal to zero. These values were determined from the kinetic curves obtained after a minimum dark period. As the dark period increases, the weights $C_i(t)$ reach equilibrium values.

Two models of environment evolution were considered.

Model of Random Changes. Model of random changes in the environment is based on the assumption that all the transitions are allowed ($W_{ij} \neq 0$ for all i and j). It is assumed that the probability of a molecule to transit from the *i*th to the *j*th ensemble is proportional to the portion of regions of *j*th type (these portions are assumed to be constant at a given temperature). This condition together with the equations of detailed balance allows expressing all the W_{ij} in term of equilibrium values of $C_i(t)$ and one parameter of transition probability, e.g., W_{12}. The equilibrium values of $C_i(t)$ and k_i were found from the kinetic curves obtained at the maximum value of τ_{dark}. The simulation procedure is described in more detail elsewhere.[41]

Numerical simulations of the isomerization kinetics using the model of random changes fail to provide adequate description of the experimental curves (the simulation results are not presented). The reason for the failure can be understood from the qualitative analysis of the kinetic curves shown in the bottom panel of Figure 4: the slowest molecules do not manifest themselves in the kinetics of isomerization at low τ_{dark} values (5−15 min). The experiment shows that the molecules populate the slowest ensemble only after sufficiently long dark pause when the intermediate ensembles are already populated. At the same time, in the framework of the model of *random changes*, the ensembles of the slowest molecules must be populated even at low values of τ_{dark}.

Model of Gradual Changes. In the context of the model of *gradual changes*, a molecule can transit from the *i*th ensemble to the adjacent ones only, i.e., $(i-1)$th or $(i+1)$th. The equations of detailed balance allow us to decrease number of free parameters W_{ij} to three, e.g., W_{12}, W_{23}, and W_{34}.

We assume that the reactivity of all the molecules of *i*th ensemble change with decrease in temperature in the same manner. It is the case when not only a molecular mobility but also some temperature dependence of the mobility can be attributed to each type of probe environment. Then, the equilibrium populations, $C_{i,eq}$ (which are established at $\tau_{dark} \to \infty$),

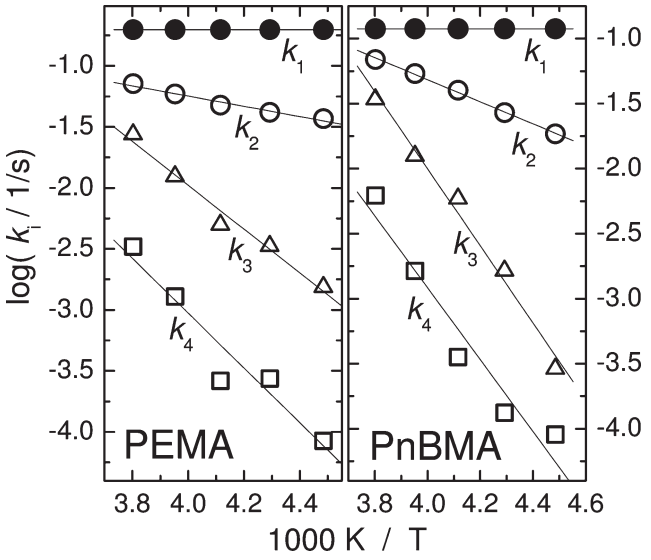

Figure 7. Temperature dependence of the effective rate constants of isomerization, k_i. The lines represent the best linear fit.

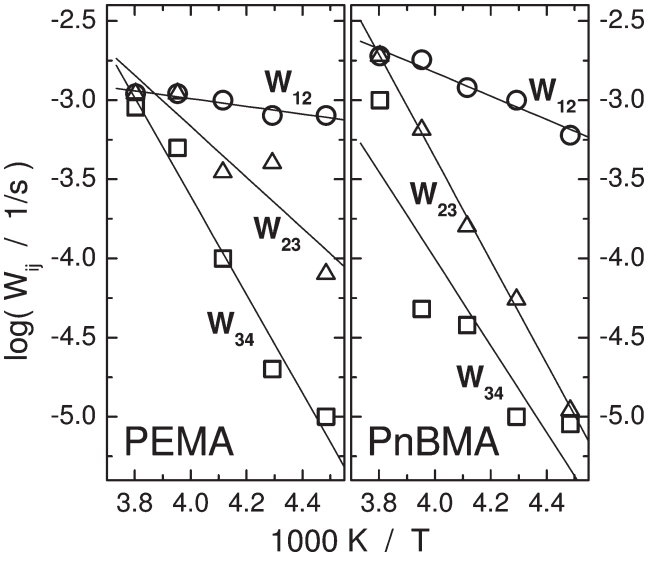

Figure 8. Temperature dependence of transition probabilities, W_{ij}. The lines represent the best linear fit.

are independent of temperature; the temperature-dependent values are $k_i(T)$ and $W_{ij}(T)$.

First, the effective rate constants of isomerization, $k_i(T)$, the initial ensemble populations, $C_i(15\ \mathrm{s})$ (at $\tau_{\mathrm{dark}} = 15$ s), and the equilibrium populations, $C_{i,\mathrm{eq}}$ (at the longest τ_{dark}), were found by simultaneous fitting of all the initial and equilibrium kinetic curves obtained at all temperatures. At that, the following conditions were used: (1) $C_3(15\ \mathrm{s}) = C_4(15\ \mathrm{s}) = 0$ (because the kinetic curves at $\tau_{\mathrm{dark}} = 15$ s are nearly exponential); (2) the effect of exchange on kinetic curve can be neglected (a case of slow exchange, i.e., $k_i \gg W_{ij}$)). The values of 0.467, 0.407, 0.083, 0.043 (PEMA) and 0.603, 0.268, 0.079, 0.05 (P*n*BMA) were obtained for the equilibrium ensemble populations, $C_{1,\mathrm{eq}}$, ..., $C_{4,\mathrm{eq}}$ respectively. The effective rate constants are presented in Figure 7.

Finally, having in hand the parameters of initial and equilibrium distributions, we determined the transition probabilities. To find W_{ij} at some temperature, all curves obtained at different τ_{dark} at this temperature were fitted simultaneously using eq 3. Usually, the parameters W_{ij} were determined from the set of 5−7 curves.

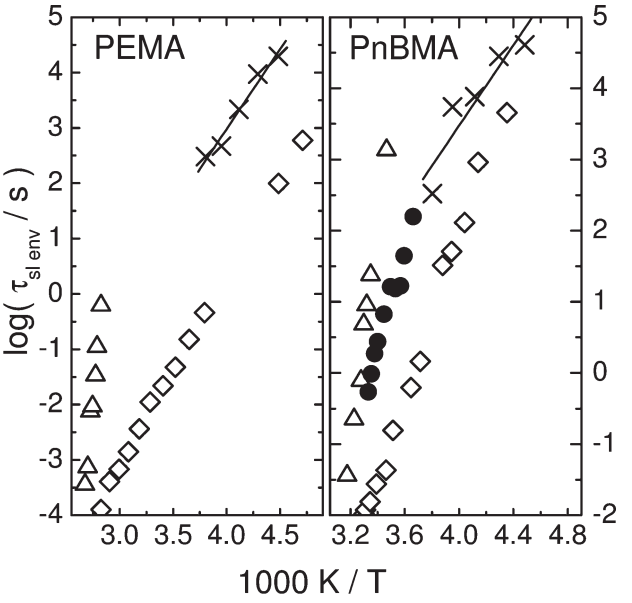

Figure 9. Temperature dependence of the lifetime of slow environments (crosses) and the times of α- (triangles) and β-relaxation (diamonds) obtained using dielectric measurements[42] and the times of α-relaxation (circles) obtained using dynamic shear modulus measurements.[30] The lines represent the best linear fit.

The model of gradual changes in the environment satisfactorily describes the evolution of probes distribution over isomerization rates in both polymer matrices. Figure 4 illustrates this by the example of NAMB isomerization in P*n*BMA. The bottom panel represents a worse description; at higher temperatures the description is better.

On the basis of the fitting results, we conclude that the conversion of the "fastest" environments into the "slowest" ones occurs not by a single step but requires a series of steps. Each step leads to only a moderate change in the environment. Note that, in contrast to the studied polymers, the exchange in low-molecular-weight glass-formers[41,47] can be described with the model of random changes in environments.

Dependence of Exchange Dynamics on Temperature. Figure 8 shows the temperature dependence of transition probabilities. The probability of transition between the two fastest environments, W_{12}, depends on temperature very slightly, whereas the transition between the two slowest ones, W_{34}, has noticeable temperature dependence. The temperature dependence of the effective rate constants, k_i, correlates with the temperature dependence of the transitions, W_{ii+1} (cf. Figures 7 and 8).

The evolution of the environment of a new-born *cis*-molecule looks like diffusion in the space of environment configurations. Being born in the point of high mobility, the system "molecule and its environment" diffuses toward the configuration of low mobility. The farther the system is from the initial point, the slower the diffusion (the environment change) and lower the isomerization rate. This process is reversible, therefore it is exactly the exchange process.

It is reasonable to assume that the isomerization of the *slowest* probes is most sensitive to the change in environment. We compared

dx.doi.org/10.1021/ma2000042 |*Macromolecules* 2011, 44, 4538–4545

the average lifetime of the two slowest environments with the literature data on times of α- and β-relaxation. The average lifetime of environments of the two slowest ensembles was determined as follows:

$$\tau_{\mathrm{sl\ env}} = \frac{C_{3,\mathrm{eq}}/(W_{32}+W_{34}) + C_{4,\mathrm{eq}}/W_{43}}{C_{3,\mathrm{eq}} + C_{4,\mathrm{eq}}}$$

The $\tau_{\mathrm{sl\ env}}$ values are plotted in Figure 9 together with the times of α- and β-relaxation obtained using dielectric spectroscopy[42] and dynamic shear modulus measurements[30] (only for PnBMA). Using the depictured data, we cannot unambiguously associate the changes in the environment of probe molecule with either α- or β-relaxation. Actually, on the one hand, the temperature dependencies of β-relaxation and of $\tau_{\mathrm{sl\ env}}$ are close each to other. The use of the Arrhenius approximation yields the activation energies for the lifetimes of slow environment of 54 ± 20 kJ/mol for P*n*BMA and of 55 ± 12 kJ/mol for PEMA. The activation energies for β-relaxation calculated using the data presented in ref 42 are 91 and 65 kJ/mol for P*n*BMA and PEMA, respectively (in the same temperature range). However, the absolute values of $\tau_{\mathrm{sl\ env}}$ and β-relaxation time differ noticeably.

The absolute values of $\tau_{\mathrm{sl\ env}}$ and α-relaxation cannot be compared directly because of the difference in temperature ranges measured. The times of α-relaxation obtained by extrapolation from the data of dielectric measurements[42] are much higher than the $\tau_{\mathrm{sl\ env}}$. However, the dielectric measurements were carried out in equilibrium matrixes while the values of $\tau_{\mathrm{sl\ env}}$ were measured using the nonequilibrium samples. In the nonequilibrium samples, the times of α-relaxation can be shorter and their temperature dependence may be less steep than that in the equilibrium ones.[30]

The times of α-relaxation in nonequilibrium P*n*BMA matrix obtained using dynamic shear modulus measurements[30] are presented in the right panel of Figure 9. The values obtained by extrapolation from these data to low temperatures looks to be closer to the $\tau_{\mathrm{sl\ env}}$ values. Additionally, the temperature dependence of α-relaxation time in nonequilibrium matrix may become weaker as temperature decreases. However, even the times of α-relaxation obtained using different methods differ widely from each other. There is no reason to consider that the times obtained using dynamic shear modulus measurements must correlate more closely with the exchange times than does the times obtained from dielectric measurements. Thus, the elucidation of the origin of change in polymer environment far below T_g requires further research.

CONCLUSIONS

Most of the probe molecules (about 85%) incorporated in P*n*BMA and PEMA matrices are located in roomy sites. The isomerization of these molecules is not affected by the environment or affected to only a small extent; their isomerization rate is the highest and does not depend on temperature or depends weakly. The rest of molecules, located, probably, in dense sites, are very sensitive to their environments and demonstrate strong temperature dependence of isomerization.

Far below T_g, the change in environment of probe molecules cannot be described by a single time parameter but requires invoking a wide range of exchange times. The time required for the environment of a molecule to change correlate with the isomerization probability of this molecule: the environment of molecules that isomerize faster changes faster.

The change in environment occurs gradually. The roomy sites are transformed into the dense ones not by a single step but through a series of steps. Each step leads to only a moderate change in the environment. As the environment becomes denser, its change with time becomes slower.

The activation energies of change in dense environments were estimated to be 54 ± 20 kJ/mol for P*n*BMA and 55 ± 12 kJ/mol for PEMA. The lifetime of roomy environments depends only weakly on temperature.

AUTHOR INFORMATION

Corresponding Author

*E-mail: grebenk@kinetics.nsc.ru.

ACKNOWLEDGMENT

The authors are grateful to Professor R. Richert for stimulating discussions and helpful advice. The authors thank Dr. B. Bol'shakov for kindly providing NAMB. This work was supported by the Russian Foundation for Basic Research, Project No. 08-03-00632-a.

REFERENCES

(1) Sillescu, H. *J. Non-Cryst. Solids* **1999**, *243*, 81–108.
(2) Ediger, M. D. *Annu. Rev. Phys. Chem.* **2000**, *51*, 99–128.
(3) Richert, R. *J. Phys.: Condens. Matter* **2002**, *14*, R703–R738.
(4) Donth, E. *J. Non-Cryst. Solids* **1982**, *53*, 325–330.
(5) Moynihan, C. T.; Schroeder, J. *J. Non-Cryst. Solids* **1993**, *160*, 52–59.
(6) Ediger, M. D. *J. Non-Cryst. Solids* **1998**, *235*−*237*, 10–18.
(7) Hempel, E.; Hempel, G.; Hensel, A.; Schick, C.; Donth, E. *J. Phys. Chem. B* **2000**, *104*, 2460–2466.
(8) Qiu, X. H.; Ediger, M. D. *J. Phys. Chem. B* **2003**, *107*, 459–464.
(9) Tracht, U.; Wilhelm, M.; Heuer, A.; Feng, H.; Schmidt-Rohr, K.; Spiess, H. W. *Phys. Rev. Lett.* **1998**, *81*, 2727–2730.
(10) Tracht, U.; Wilhelm, M.; Heuer, A.; Spiess, H. W. *J. Magn. Reson.* **1999**, *140*, 460–470.
(11) Reinsberg, S. A.; Qiu, X. H.; Wilhelm, M.; Spiess, H. W.; Ediger, M. D. *J. Chem. Phys.* **2001**, *114*, 7299–7302.
(12) Reinsberg, S. A.; Heuer, A.; Doliwa, B.; Zimmermann, H.; Spiess, H. W. *J. Non-Cryst. Solids* **2002**, *307*−*310*, 208–214.
(13) Schmidt-Rohr, K.; Spiess, H. W. *Phys. Rev. Lett.* **1991**, *66*, 3020–3023.
(14) Heuer, A.; Wilhelm, M.; Zimmermann, H.; Spiess, H. W. *Phys. Rev. Lett.* **1995**, *75*, 2851–2854.
(15) Böhmer, R.; Hinze, G.; Diezemann, G.; Geil, B.; Sillescu, H. *Europhys. Lett.* **1996**, *36*, 55–60.
(16) Kuebler, S. C.; Heuer, A.; Spiess, H. W. *Phys. Rev. E* **1997**, *56*, 741–749.
(17) Hinze, G.; Diezemann, G.; Sillescu, H. *Europhys. Lett.* **1998**, *44*, 565–570.
(18) Hinze, G. *Phys. Rev. E* **1998**, *57*, 2010–2018.
(19) Tracht, U.; Heuer, A.; Reinsberg, S. A.; Spiess, H. W. *Appl. Magn. Reson.* **1999**, *17*, 227–241.
(20) Qi, F.; Schug, K. U.; Dupont, S.; Döss, A.; Böhmer, R.; Sillescu, H.; Kolshorn, H.; Zimmermann, H. *J. Chem. Phys.* **2000**, *112*, 9455–9462.
(21) Vidal Russell, E.; Israeloff, N. E. *Nature* **2000**, *408*, 695–698.
(22) Wang, C.-Y.; Ediger, M. D. *J. Phys. Chem. B* **1999**, *103*, 4177–4184.
(23) Cicerone, M. T.; Ediger, M. D. *J. Chem. Phys.* **1995**, *103*, 5684–5692.
(24) Wang, C.-Y.; Ediger, M. D. *J. Chem. Phys.* **2000**, *112*, 6933–6937.

(25) Deschenes, L. A.; Vanden Bout, D. A. *J. Phys. Chem. B* **2002**, *106*, 11438–11445.
(26) Schob, A.; Cichos, F.; Schuster, J.; von Borczyskowski, C. *Eur. Polym. J.* **2004**, *40*, 1019–1026.
(27) Adhikari, A. N.; Capurso, N. A.; Bingemann, D. *J. Chem. Phys.* **2007**, *127*, 114508−1–114508−9.
(28) Zondervan, R.; Kulzer, F.; Berkhout, G. C. G.; Orrit, M. *Proc. Natl. Acad. Sci. U.S.A.* **2007**, *104*, 12628–12633.
(29) Mackowiak, S. A.; Herman, T. K.; Kaufman, L. J. *J. Chem. Phys.* **2009**, *131*, 244513−1–244513−14.
(30) Beiner, M.; Garwe, F.; Schröter, K.; Donth, E. *Colloid Polym. Sci.* **1994**, *272*, 1439–1446.
(31) Beiner, M.; Garwe, F.; Schröter, K.; Donth, E. *Polymer* **1994**, *35*, 4127–4132.
(32) Schiener, B.; Chamberlin, R. V.; Diezemann, G.; Böhmer, R. *J. Chem. Phys.* **1997**, *107*, 7746–7761.
(33) Richert, R. *J. Chem. Phys.* **2001**, *115*, 1429–1434.
(34) *Photoreactive Organic Thin Films*; Sekkat, Z., Knoll, W., Eds.; Academic Press: San Diego, 2002.
(35) Victor, J. G.; Torkelson, J. M. *Macromolecules* **1988**, *21*, 3490–3497.
(36) Yu, W.-C.; Sung, C. S. P.; Robertson, R. E. *Macromolecules* **1988**, *21*, 355–364.
(37) Mita, I.; Horie, K.; Hirao, K. *Macromolecules* **1989**, *22*, 558–563.
(38) Richert, R. *Macromolecules* **1988**, *21*, 923–929.
(39) Richert, R.; Heuer, A. *Macromolecules* **1997**, *30*, 4038–4041.
(40) Park, J.-W.; Ediger, M. D.; Green, M. M. *J. Am. Chem. Soc.* **2001**, *123*, 49–56.
(41) Grebenkin, S. Y. *J. Phys. Chem. B* **2008**, *112*, 15369–15375.
(42) Garwe, F.; Schönhals, A.; Lockwenz, H.; Beiner, M.; Schröter, K.; Donth, E. *Macromolecules* **1996**, *29*, 247–253.
(43) Schröter, K.; Unger, R.; Reissig, S.; Garwe, F.; Kahle, S.; Beiner, M.; Donth, E. *Macromolecules* **1998**, *31*, 8966–8972.
(44) Beiner, M. *Macromol. Rapid Commun.* **2001**, *22*, 869–895.
(45) Arbe, A.; Genix, A.-C.; Arrese-Igor, S.; Colmenero, J.; Richter, D. *Macromolecules* **2010**, *43*, 3107–3119.
(46) Becker, H.; *Organicum*, 15th ed.; VEB Deutscher Verlag der Wissenschaften: Berlin, 1976.
(47) Grebenkin, S. Y.; Syutkin, V. M. *Phys. Rev. B* **2007**, *76*, 054202-1–054202-6.